Chinese Chemical Letters 34 (2023) 108040

Contents lists available at ScienceDirect

Chinese Chemical Letters

journal homepage: www.elsevier.com/locate/cclet

Supramolecular assemblies of cucurbit[*n*]urils and 4-aminopyridine controlled by cucurbit[*n*]uril size (*n* = 5, 6, 7 and 8)

Yun Lu[a,1], Zhichao Yu[a,1], Xinan Yang[a], Jingjing Dai[a], Peihui Shan[a], Xianhao Feng[a], Zhu Tao[a], Carl Redshaw[b], Xin Xiao[a,*]

[a] Key Laboratory of Macrocyclic and Supramolecular Chemistry of Guizhou Province, Guizhou University, Guiyang 550025, China
[b] Department of Chemistry, University of Hull, Hull HU6 7RX, United Kingdom

ARTICLE INFO

Article history:
Received 28 August 2022
Revised 1 December 2022
Accepted 1 December 2022
Available online 5 December 2022

Keywords:
Cucurbit[*n*]urils
4-Aminopyridine
Host-guest chemistry
Supramolecular assembly
Exo binding

ABSTRACT

The binding interactions between 4-aminopyridine (4-AP) and a series of cucurbit[*n*]urils (Q[5], Q[6], TMeQ[6], Q[7], Q[8]) have been studied using ^{1}H NMR spectroscopy, UV–vis absorption spectroscopy, isothermal titration calorimetry (ITC) and X-ray crystallography. The data indicates that the Q[5]@4-AP complex exhibits *exo* binding, which is not observed in the other four host-guest complexes. Furthermore, X-ray crystallography clearly reveals how the Q[*n*]s bind with 4-AP to form complexes, for example Q[5] forms an outer-surface complex, whilst Q[6], TMeQ[6] and Q[7] formed 1:1 host and guest type complexes, and Q[8] formed a stable 1:2 ternary complex due to its large cavity, which can accommodate two 4-AP molecules.

4-Aminopyridine (4-AP), also known as aminopyridine or 4-pyridine amine, is commonly used as a pesticide, in medicine and as a dye intermediate. 4-Aminopyridine is a potassium channel blocker that has clinical advantages in patients with MS (Multiple Sclerosis), particularly for improving visual function [1], fatigue [2], cognitive [3], and walking speed. However, 4-aminopyridine and its positional isomers, 2-aminopyridine and 3-aminopyridine, are all aromatic amines (anilines), and their structures are flagged with a genotoxic warning [4,5]. Indeed, the toxicological data and environmental behavioral toxicity of 4-aminopyridine puts it in the highly toxic class. It has been shown to possess high toxicity toward animals [6]. Given that 4-AP has a unique structure and chemical properties, many domestic pharmaceutical manufacturers utilize it as an important intermediate of synthetic drugs and chemical raw materials [7]. On the other hand, 4-AP has an amino group and a pyridine group. The amino group is the hydrogen bond donor, and the pyridine group is the hydrogen bond acceptor. It is a good guest molecule for host-guest complexation.

In recent years, host-guest complexation has gained increasing attention. Cucurbit[*n*]urils (Q[*n*]s, *n* = 5–8, 10 and 13–15), are a class of macrocyclic hosts with special structural, possessing glycoluril units bridged by methylene groups, a hydrophobic pumpkin-shaped cavity with different sizes, two polar carbonyl portals rimmed with numerous carbonyl oxygen groups, and a positive charged outer surface [8–11]. Thanks to their structural characteristics, the neutral rigid hydrophobic cavities facilitate the binding of guest molecules through hydrophobic interactions to form the host-guest inclusion complexes [12–22]. Q[*n*]s with different degrees of polymerization have cavities of different sizes, and these are capable of capturing one or two hydrophobic guest molecules or groups of appropriate size and shape. Their two identical carbon-based inlets make them attractive coordination ligands. Two negative electrostatic portals promote the coordination of metal cations to form coordination complexes *via* ion-dipole interactions [23–28]. Compared with other macrocyclic hosts, such as cyclodextrins, pillar[*n*]arenes, and calix[*n*]arenes [29,30], Q[*n*]s possess a hydrophobic cavity with different sizes and different binding affinities. They exhibit excellent properties both in solution and the solid state [31,32], especially in terms of selectivity and affinity in aqueous solution. These excellent properties are attributed to their special structures [33–35] and the corresponding macrocyclic-confinement effect. The hydrophobic cavities associated with the Q[*n*]s play a central role in their host-guest complexation.

Given this, we sought to explore how the cavity size of the Q[*n*]s affects the host-guest binding patterns. A range of host-guest supramolecular structures comprising different Q[*n*]s and 4-aminopyridine (4-AP) were constructed, including systems employing Q[5], Q[6], TMeQ[6], Q[7] and Q[8]. The interactions of

* Corresponding author.
E-mail address: gyhxxiaoxin@163.com (X. Xiao).
[1] These authors contributed equally to this work.

https://doi.org/10.1016/j.cclet.2022.108040
1001-8417/

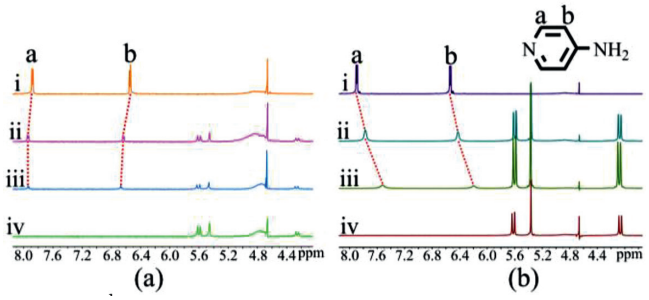

Fig. 1. (a) ^{1}H NMR spectra of 4-AP (i) in the absence of Q[5]; (ii) in the presence of 0.20; (iii) 0.49 equiv. of Q[5] and (iv) neat Q[5] in D_2O at 20 °C. (b) ^{1}H NMR spectra of 4-AP (i) in the absence of Q[7]; (ii) in the presence of 0.33; (iii) 1.10 equiv. of Q[7] and (iv) neat Q[7] in D_2O at 20 °C.

4-aminopyridine and the Q[*n*]s (Q[5], Q[6], TMeQ[6], Q[7] and Q[8]) were explored using UV–vis spectroscopy, ^{1}H NMR spectroscopy, isothermal titration calorimetry (ITC) and X-ray diffraction. The host-guest interaction of the Q[*n*] depends mainly on the cavity, so the interaction of the smaller member, Q[5] with 4-AP was first investigated. The unsubstituted Q[5] is the smallest member of the Q[*n*]s families and its smaller cavity inhibits the entry of most molecules, thereby reducing the possibility of Q[5]-inclusion-complexes. Herein, we selected the guest 4-AP, and this formed a Q[5]-outer-surface complex. The host-guest interaction of the larger homologs Q[6], TMeQ[6], Q[7] and Q[8] with 4-AP were subsequently studied. Q[6], TMeQ[6] and Q[7] with 4-AP formed 1:1 host and guest complexes, while Q[8] formed a stable 1:2 ternary complex due to its large cavity, which can accommodate two 4-AP molecules.

To explore the binding behavior between Q[*n*]s (Q[5], Q[6], TMeQ[6], Q[7] and Q[8]) and 4-AP, ^{1}H NMR spectroscopic titration experiments were performed. The first complex studied, namely Q[5]@4-AP complex exhibits *exo* binding, which is not observed in the other four host-guest complexes. As shown in Fig. 1a, upon addition of increasing amounts of Q[5], the two protons H_a and H_b on the pyridine group of the guest underwent a slight downfield shift of 0.06 ppm (from 7.88 ppm to 7.94 ppm) and 0.12 ppm (from 6.54 ppm to 6.66 ppm) compared to unbound 4-AP. These observations indicated that the 4-AP was located outside the cavity of the Q[5] to form the exclusion complex Q[5]@4-AP.

As shown in Fig. S1 (Supporting information), on gradual addition of Q[6], the two protons on the pyridine (H_a, H_b) were split into two signals respectively. Both the signals of the proton Ha underwent a gradual upfield shift, while part of the signals of proton H_b exhibited a downfield shift. These phenomena suggested that H_a and H_b of the 4-AP were located in a different chemical environment from the unbound 4-AP. Both binding modes of 4-AP and Q[6] existed simultaneously in solution. One is that 4-AP was completely encapsulated into the cavity of Q[6], which was consistent with the crystal structure in the solid state. Another may be that the proton H_a of 4-AP close to pyridine nitrogen was encapsulated into the cavity, while the proton H_b close to amino was located at the port of Q[6], and there are hydrogen bonds between H_b and the carbonyl oxygen atoms of the port. Similar to the Q[6]@4-AP system, as shown in Fig. S2 (Supporting information), titration of 4-AP into TMeQ[6] resulted in similar observations. The cavity of TMeQ[6] is similar to that of Q[6] in size, so in solution, 4-AP and TMeQ[6] also persisted with two bonding modes simultaneously. The exploration of the binding behavior of 4-AP with the larger Q[7] as compared to Q[6] and TMeQ[6] showed completely different results. As shown in Fig. 1b, on account of the shielding from the Q[7] cavity, the resonances of protons H_a and H_b of 4-AP underwent a dramatic upfield shift of 0.38 ppm (from 7.90 ppm to 7.52 ppm), 0.35 ppm (from 6.55 ppm to 6.20 ppm), suggesting that the 4-AP was accommodated within the Q[7] cavity to form an inclusion complex. Complexation of 4-AP with Q[8] also led to upfield shifts of the proton signals of 4-AP in the ^{1}H NMR spectra, as shown in Fig. S3 (Supporting information). An upfield shift of the protons H_a and H_b on the pyridine was observed, which suggested that 4-AP was deeply encapsulated in the Q[8] cavity to form an inclusion complex.

The interaction between 4-AP and Q[*n*]s was further explored using UV–vis spectroscopy. As illustrated in Fig. 2 and Figs. S4-S7 (Supporting information), four of the systems exhibit similar phenomena, whilst the system Q[5]@4-AP behaved differently. Complexes of 4-AP with Q[6], TMeQ[6], Q[7] and Q[8] led to changes in the UV–vis spectra of the guest, while for Q[5], no significant variations of the UV–vis spectra of 4-AP were observed (Fig. S4). In the case of Q[6], TMeQ[6] and Q[7], Fig. 2, Figs. S5 and S6 show that 4-AP displayed an absorption peak at 262 nm in aqueous solution. As the concentration of the Q[*n*]s increased in the guest solution (at a fixed 4-AP concentration of 2.0×10^{-5} mol/L), the absorption band of the guest displayed progressively lower absorbance until the ratio of the host-guest reached 1.0. A stoichiometric analysis (Jobs plot) revealed a 1:1 stoichiometry for the host and guest complexes. In the case of Q[8], as shown in Figs. S7a and b, the decreasing absorbance of the 4-AP in the presence of increasing amounts of Q[8] indicated the formation of the host-guest complex Q[8]@4-AP. The absorbance reached a minimum at an $N_{Q[8]}/N_{4\text{-AP}}$ ratio of 1:2. The Jobs plot further indicated that a 1:2 ternary complex (Q[8]/4-AP) was formed (Fig. S7c).

To explore the thermodynamic parameters and to shed light on the thermal stability and driving force of the interactions, ITC experiments were performed at 298.15 K in pure water. Computer simulations (curve fitting) based on microcalorimetric titration data using Nano ITC analysis software gave the associated thermodynamic parameters. The smaller cavity of Q[5] inhibits the entry of 4-AP into it, so Q[5] and 4-AP do not form an exclusion complex. Table 1 shows that the other four systems exhibit high binding strengths ($K_a > 10^4$ L/mol) confirming the thermodynamic stability of the host-guest (including Q[6], TMeQ[6], Q[7] and Q[8]

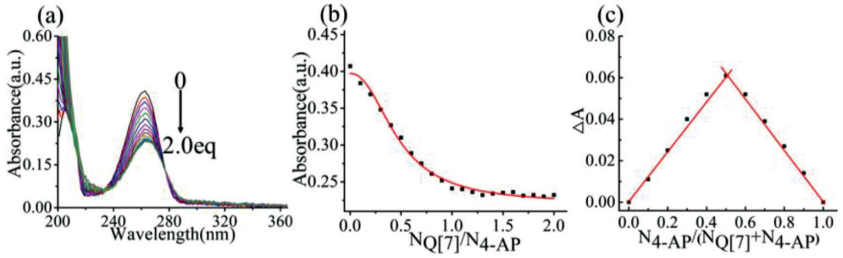

Fig. 2. (a) UV–vis spectral changes of 4-AP (2.0×10^{-5} mol/L) upon stepwise addition of 0~2.0 equiv. Q[7] in aqueous solution at 298 K; (b) The corresponding absorbance changes at 262 nm *vs.* $N_{Q[7]}/N_{4\text{-AP}}$; (c) Jobs plot for Q[7] and 4-AP in water by recording the absorbance changes at 262 nm.

Table 1
Data obtained from ITC experiments.

Host–guest	K_a (L/mol)	ΔH (kJ/mol)	$T\Delta S$ (kJ/mol)	ΔG (kJ/mol)
Q[6]–4-AP	1.115×10^5	−100.00	−71.73	−28.27
TMeQ[6]–4-AP	1.694×10^6	−42.66	−9.72	−32.94
Q[7]–4-AP	6.022×10^6	−18.29	11.51	−6.78
Q[8]–4-AP	3.684×10^9 (M^{-2})	−371.80	−317.50	−54.30

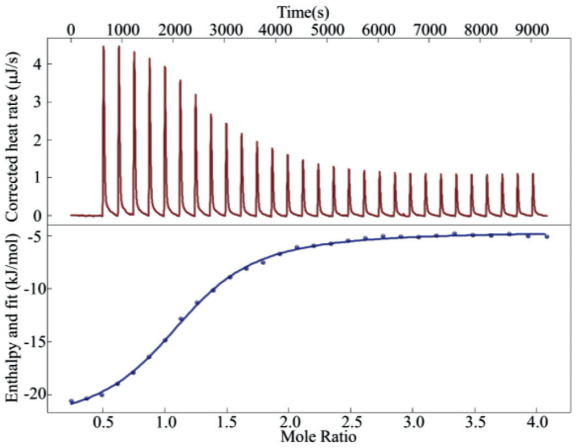

Fig. 3. ITC isotherm obtained by titrating 4-AP with Q[7] in aqueous solution.

with 4-AP) except for the system Q[5]@4-AP. As shown in Fig. 3 and Figs. S8-S10 (Supporting information), the four binding curves with a clear transition indicate the successful incorporation of 4-AP into the Q[*n*]s (Q[6], TMeQ[6], Q[7] and Q[8]). From the ΔH and $T\Delta S$ values, the observed negative enthalpy change (ΔH) of these four systems is probably due to the contribution of the hydrophobic effect between the cavity of Q[*n*]s and 4-AP. Furthermore, the enthalpy changes indicated that the bindings between the Q[*n*]s and the guest were mainly driven by enthalpy in these four systems. As shown in Table 1, the binding constant (K_a) for the complexation of Q[6] with 4-AP was found to be 1.115×10^5 L/mol, indicating a moderate binding constant. Similar ITC results were obtained for TMeQ[6] and 4-AP, Q[7] and 4-AP, while the larger K_a values (1.694×10^6 L/mol, 6.022×10^6 L/mol) suggested that after encapsulating the 4-AP in the TMeQ[6], Q[7] cavity, a supramolecular complex was formed with a stable binding constant. The experimental results indicated that their binding constants were in between the binding strengths of Q[6] and Q[8]. Complexation by the Q[8] host and 4-AP formed the supramolecular complex Q[8]@4-AP with an expected high binding constant (3.684×10^9 M^{-2}), which suggested that the Q[8]@4-AP complex is more stable than other four systems.

In order to further obtain direct information of the binding interactions of 4-AP with Q[*n*]s (Q[5], Q[6], TMeQ[6], Q[7] and Q[8]), we also attempted to obtain single crystals by slow evaporation of the HCl solutions of Q[*n*]s and 4-AP. The detailed crystallographic data of the five complexes are listed in Table S1 (complex **1**: Q[5]@4-AP; complex **2**: Q[6]@4-AP; complex **3**: TMeQ[6]@4-AP; complex **4**: Q[7]@4-AP; complex **5**: Q[8]@4-AP). The crystal data have been deposited in the Cambridge Crystal Data Center under accession numbers CCDC: 2191294, 2190281, 2190283, 2190282 and 2190285 for complex **1**–**5**, respectively.

The asymmetric unit of complex **1** contains one half-Q[5] host molecule, one protonated 4-aminopyridine molecule, one Zn^{2+} ion, one coordination water molecule and two $[ZnCl_4]^{2-}$ anion (Fig. S11a in Supporting information). The Zn^{2+} ion of the complex is six coordinate octahedral, and is coordinated with two water molecules (O6 and $O6^{ii}$) and four carbonyl oxygen atoms

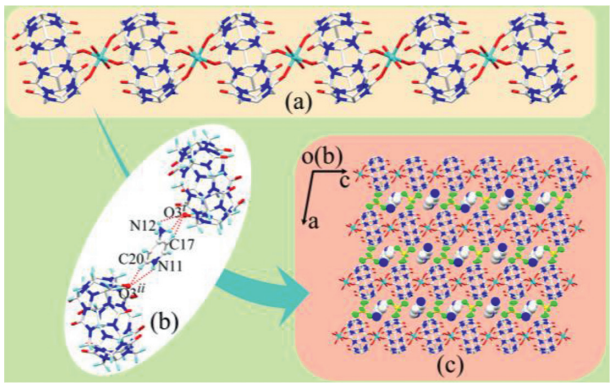

Fig. 4. (a) One-dimensional supramolecular chain of **1**; (b) Hydrogen-bonding interactions between the 4-AP and Q[5] host; (c) Two-dimensional structure of **1** viewed down the *b* axis.

(O4, $O5^{i}$, $O4^{ii}$ and $O5^{iii}$) of the Q[5] host (where $i = 1-x, +y, 3/2-z$, $ii = 1-x, 1-y, 1-z$, $iii = +x, 1-y, -1/2+z$). The interaction distances of Zn1–O6($O6^{ii}$), Zn1–O4($O4^{ii}$) and Zn1–$O5^{i}$($O5^{iii}$) are 2.024(6) Å, 2.096(5) Å and 2.148(6) Å, respectively (Fig. S11b in Supporting information). There are hydrogen bonds between the coordinated water molecules and the carbonyl oxygen atom of the Q[5] host. Further analysis of the structure of **1** reveals that each portal of the Q[5] molecule is coordinated with a Zn^{2+} ion, while each Zn^{2+} ion coordinates with two adjacent Q[5] molecules. Thus a one-dimensional Q[5]-Zn^{2+} coordination polymer/chain structure was formed (Fig. 4a).

Different from other complexes, the guest molecule 4-AP in **1** interacts with the outer surface of the Q[5] rather than inside it. As shown in Fig. 4b, N12 and C17 on the 4-AP interacts with the carbonyl oxygen atom $(O3)^{i}$ of the Q[5] host *via* hydrogen bonding; N11 and C20 also interacts with the carbonyl oxygen atom $(O3)^{ii}$ of another Q[5] *via* hydrogen bonds (where $i = 1-x, +y, 3/2-z$, $ii = 1-x, 1-y, 1-z$). At the same time, the interaction distances are N(12)–H(12B)···$O(3)^{i}$, N(12)–H(12C)···$O(3)^{i}$, C(17)–H···$O(3)^{i}$, N(11)–H···$O(3)^{ii}$ and C(20)–H···$O(3)^{ii}$ are 2.707(6) Å, 2.303(6) Å, 2.989(7) Å, 3.148(6) Å and 2.597(7) Å, respectively. Under the action of 4-AP bridging, the one-dimensional supramolecular chain is promoted to form a two-dimensional layered supramolecular structure, in which the $[ZnCl_4]^{2-}$ anions were arranged regularly between layers (Fig. 4c).

The crystal structure of **2** reveals that it crystallized in the monoclinic crystal system with the $P2_1/c$ space group. As shown in Fig. 12a (Supporting information), the asymmetric unit of the complex includes half of the Q[6] host, one protonated 4-aminopyridine molecule, one protonated water molecule, two lattice water molecules, and one $[ZnCl_4]^{2-}$ anion. The protonated guest molecules are encapsulated in the center of the Q[6] cavity and are nearly perpendicular to the mean plane of the six carbonyl oxygen atoms of the Q[6] portal, while the ammonium group molecules are almost in that plane. In Fig. 12b (Supporting information), the encapsulated guest 4-aminopyridine forms multiple hydrogen-bonds with the host Q[6]: one proton of the ammonium group forms two hydrogen bonds with the carbonyl atoms (O4 and C13) of the Q[6] host at an N(13)–H···O(4) distance of 2.128(4) Å and N(13)–H···C(13) distance of 2.805(5) Å. The hydrogen-bonding interactions between the carbon atoms (C20, C22 and C23) of the pyridyl with the Q[8] host exhibit distances of C(20)–H···C(11) 2.736(4) Å, C(22)–H···O(6) 2.458(4) Å, C(22)–H···C(17) 2.669(5) Å, C(23)–H···$C(11)^{i}$ 2.343(4) Å, C(23)–H···$N(11)^{i}$ 2.654(4) Å, and C(23)–H···$N(12)^{i}$ 2.410(4) Å, where $i = 1-x, 1-y, 1-z$.

Further analysis of the crystal structure of **2** reveals extensive hydrogen bonding between the different complexes. In Fig.

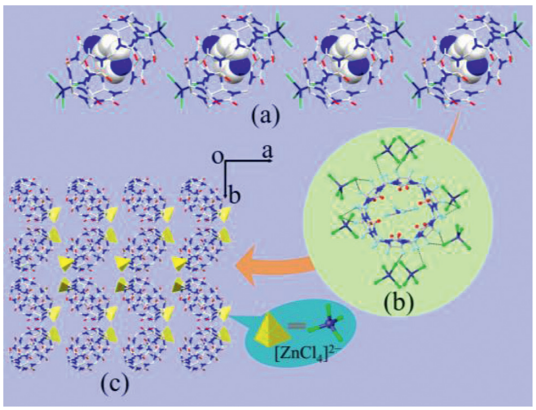

Fig. 5. (a) One-dimensional supramolecular chain of **2**; (b) Detailed ion-dipole interaction between **2** and $[ZnCl_4]^{2-}$ anions; (c) Two-dimensional structure of **2** viewed down the *c* axis.

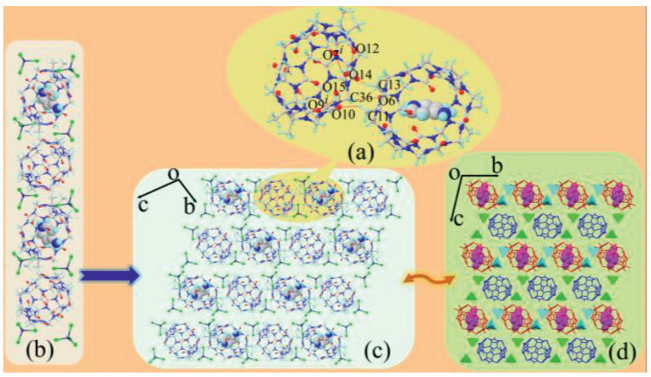

Fig. 6. (a) Hydrogen-bonding interactions between the TMeQ[6]@4-AP; (b) One-dimensional supramolecular chain of **3**; (c, d) Two-dimensional structure of **3** viewed down the *a* axis.

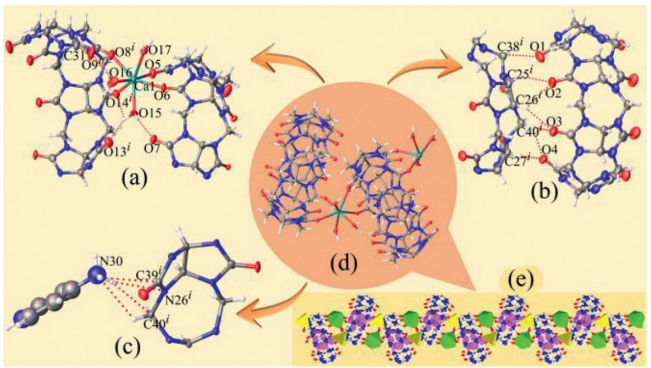

Fig. 7. (a-c) Detailed interactions between adjacent complexes; (d) Interactions between **4**. (e) One-dimensional supramolecular chain of **4**.

12c (Supporting information), the methylene groups of one complex formed hydrogen bonds with water molecules (O7 and O8) and these water molecules formed hydrogen bonds with the carbonyl oxygen of another complex. A hydrogen bonded network: C(4)^i···O(8)···O(5), C(4)^i···O(8)···O(4), C(4)^i···O(8)···O(7)···O(3), C(14)^i···O(7)···O(3), C(14)^i···O(7)···O(8)···O(5) was observed with bond lengths between 2.104(3) and 2.672(10) Å, where $i = 1\text{-}x$, 1-*y*, 1-*z*. Moreover, each $[ZnCl_4]^{2-}$ anion forms strong C–H···Cl contacts with four Q[6] hosts *via* ion-dipole interactions (Fig. 12d in Supporting information). Each inclusion complex Q[6]@4-AP is surrounded by eight tetrahedral $[ZnCl_4]^{2-}$ counterions (Fig. 5b). As a result, driven by these weak interactions (hydrogen bonding and ion-dipole interactions), the complex Q[6]@4-AP forms an orderly multidimensional layered supramolecular structure (Fig. 5c, Figs. S13a and b in Supporting information).

Complex **3** crystallized in the triclinic crystal system, with the space group *P*-1. As shown in Fig. S14a (Supporting information), there are two crystallographically independent half-TMeQ[6] hosts in the asymmetric unit, one of which contains the 4-AP molecule and the other is empty. One 4-AP molecule was observed to be encapsulated into the small hydrophobic cavity of TMeQ[6] (Fig. S14b in Supporting information). One proton of the ammonium group forms a hydrogen bond with the carbonyl oxygen atom O5 of the TMeQ[6] host with an N(26)–H···O(5) distance of 2.362(4) Å and an N(26)–H···O(6) distance of 2.040(3) Å. There are abundant hydrogen bonds between the carbon atoms (C41, C42, C44 and C45) of the pyridyl and the TMeQ[6] host (C41···N5^i, C41···N11^i, C42···O2^i, C42···O3^i, C44···O6, C44···N11 and C45···O3 distances in the range 2.172(3)–2.787(3) Å, where $i = 1\text{-}x$, 1-*y*, -*z*).

Compared with complex **2**, the substituted methyl groups on the waist of the TMeQ[6] enrich the hydrogen presence on the outer surface, facilitating the easier formation of hydrogen bonds between adjacent TMeQ[6] molecules. At the same time, the methyl groups belong to electron-donating groups, which can enhance the polar properties of the carbonyl oxygen atoms at the portal, and might be profitable to enhance the electrostatic interactions between TMeQ[6] and metal ions. As shown in Fig. 6a, hydrogen bonding is formed directly or indirectly between the TMeQ[6] host of the inclusion complex **3** and the adjacent empty TMeQ[6] host, *e.g.*, C(11)–H···O(10), C(36)–H···O(6), C(13)···O(14)···O(7)^i, C(13)···O(14)···O(12) were observed with bond lengths between 1.912(3) and 2.795(3) Å, where $i = -x, 2-y, 1-z$. A one-dimensional supramolecular chain is thus formed, driven by these hydrogen bonding interactions (Fig. 6b). Meanwhile, each $[ZnCl_4]^{2-}$ anion forms a strong C–H···Cl contacts with adjacent TMeQ[6] hosts *via* ion-dipole interactions. Overall, complex **3** forms a layered supramolecular structure with different shapes along the *a*-axis (Figs. 6c and d), in which the $[ZnCl_4]^{2-}$ anions are arranged regularly between layers.

Complex **4** crystallizes in the monoclinic space group $P2_1/n$ and the asymmetric unit contains one Ca^{2+} and one Q[7]@4-AP molecule, three coordinated water molecules and two $[CdCl_4]^{2-}$ anions. The angle between the plane where the guest molecule is located and the plane established by the seven carbonyl oxygen atoms of the Q[7] host is 55.67° (Fig. S15a in Supporting information). A calcium ion coordinates with the carbonyl oxygen atoms (O5 and O6) in the port of Q[7] in Q[7]@4-AP, where the distances from Ca1 to O5 and O6 are 2.377(6) and 2.409(5) Å respectively, and there are three molecules (O15, O16, O17) of water bound to Ca1. The center of symmetry generates another Q[7] and guest. The second Q[7] binds to the Ca1 *via* O(8)^i and O(14)^i (Ca1–O(8)^i and Ca1–O(14)^i is 2.411(6) and 2.382(5) Å respectively, where $i = 3/2-x,\ 1/2+y,\ 1/2-z$), so that each Ca^{2+} is 7-coordinate. As shown in Fig. S15b (Supporting information), the Q[7] and protonated 4-aminopyridine form a 1:1 assembly *via* hydrogen bonds, where the protonated ammonium group forms multiple hydrogen bonds with C3, N3, O1 and O2 of the Q[7]; the bond lengths of these hydrogen bonds are between 2.191 (8) and 2.701 (8) Å. Moreover, the hydrogen-bonding interaction between the carbon atom C43 of the pyridyl with the Q[7] host exhibit distances of C(43)–H···C(39) 2.651(7) Å.

Further inspection of the crystal structure of **4** reveals that two adjacent complexes form an interesting wavy one-dimensional supramolecular chain under the guidance of Ca^{2+} (Fig. 7e). Fig. 7c shows that the 4-aminopyridine in one complex not only forms hydrogen bonds with the Q[7] host, but also with the

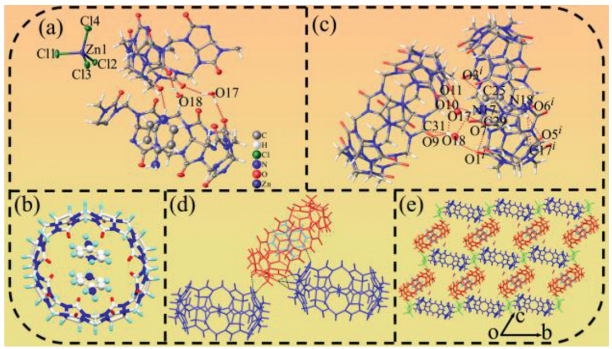

Fig. 8. (a) Asymmetric unit of **5**; (b) Molecular structure of Q[8]@4-AP; (c) Hydrogen-bonding interactions between the guest molecule and Q[8] host; (d) Hydrogen-bonding interactions between the Q[8]@4-AP; (e) Two-dimensional grid-like structure of **5** viewed down the *a* axis.

Q[7] host in the adjacent complex. These hydrogen bonds—*i.e.,* N(30)–H···C(39)^{i}, N(30)–H···C(40)^{i}, N(30)–H···N(26)^{i} and C(40)^{i}–H···N(30)—have bond lengths of 2.894(7), 2.440(7), 2.679(6) and 2.740(3) Å, respectively, where $i = 3/2 - x,\ 1/2 + y,\ 1/2 - z$. In addition, there is also hydrogen-bonding between the coordinated water molecules (O15 and O16) and Q[7] (Fig. 7a). At the same time, the neighboring Q[7] hosts interact with carbonyl oxygens of neighboring Q[7] hosts *via* C–H···O hydrogen bonding between the methine or methylene groups at the outer surface of the Q[7] host (Fig. 7b). In summary, **4** forms an ordered two-dimensional supramolecular structure in the presence of multiple forces (Fig. S16 in Supporting information).

Single crystal X-ray diffraction analysis reveals that complex **5** crystallizes in the triclinic crystal system, with space group *P*-1. As shown in Fig. 8a, there are two crystallographically independent half-Q[8] hosts in the asymmetric unit, one protonated 4-aminopyridine molecule, along with one single $[ZnCl_4]^{2-}$ ion and two lattice water molecules. The inclusion of guests by the macrocycle is shown in Fig. 8b, one Q[8] host has encapsulated two 4-aminopyridine molecules in an off-set centrosymmetric embrace. The planar spacing between the two guest molecules is 3.839 Å, the other accommodates some disordered water molecules or is empty. As shown in Fig. 8c, the encapsulated guest 4-aminopyridine forms multiple hydrogen-bonds with the host Q[8] or solvent water molecules. The hydrogen-bonding interactions between the carbon atoms of the pyridyl with the portal carbonyl oxygen atoms of Q[8] exhibit distances of C(29)–H···O(1)^{i} 2.558(8) Å and C(25)–H···O(3)^{i} 2.557(7) Å, where $i = 1 - x,\ 1 - y,\ 1 - z$. The protonated nitrogen atom forms hydrogen bonds with the solvent water molecule and another empty Q[8] carbonyl oxygen atom O10, with an N(17)–H···O(18) distance of 2.704(6) Å and N(17)–H···O(10) distance of 1.947(5) Å. Meanwhile, the protons of the ammonium group also form multiple hydrogen bonds with the Q[8] host (N···O and N···C distances in the ranges of 2.420(6)–2.756(9) Å). Moreover, in the complex Q[8]@4-AP, the Q[8] host of the inclusion complex Q[8]@4-AP forms hydrogen bonds with a water molecule, which also forms hydrogen bond with another empty Q[8] host. Hydrogen bonding bridges, such as O(7)···O(17)···O(11), O(1)^{i}···O(18)···O(9), O(1)^{i}···O(18)···C(31), O(1)^{i}···O(18)···O(10), were observed with bond lengths between 1.652(6) and 2.771(9) Å, where $i = 1 - x,\ 1 - y,\ 1 - z$. Interestingly, each empty Q[8] host forms multiple C–H···O hydrogen bonds with four neighboring inclusion complexes Q[8]@4-AP. At the same time, the Q[8] host of the inclusion complex Q[8]@4-AP also interacts with four empty Q[8] hosts through C–H···O hydrogen bonding. In such a way, they form a two-dimensional grid-like structure parallel to the *b*, *c*-plane of the unit cell, as shown in Fig. 8e. This stacking of the grid-like structure creates multiple one-dimensional channels along the *a*-axis, in which the $[ZnCl_4]^{2-}$ anions and water molecules were entrapped. It is interesting to compare the modes of action of these five inclusion complexes. The binding interaction of the host Q[5] and the other cucurbit[*n*]urils (Q[6], TMeQ[6], Q[7] and Q[8]) with the 4-AP reveals two different binding modes (*exo* and *endo* binding). Q[6], Q[7] and TMeQ[6] all accommodate one guest molecule, whilst Q[8], where there is a spacious hydrophobic cavity, accommodates two guest molecules.

In summary, we have investigated the binding interactions between 4-aminopyridine (4-AP) and a series of cucurbit[*n*]urils (Q[5], Q[6], TMeQ[6], Q[7] and Q[8]), both in the solid state and in aqueous solution. All the characterization results indicate that the hydrophobic cavities associated with the Q[*n*]s play a central role in their host-guest complexation. The different size of the cavity of the Q[*n*]s determines the binding interactions between 4-AP and each Q[*n*]s. The Q[5]@4-AP complex exhibits *exo* binding, which is not observed in the other four host-guest complexes. Furthermore, X-ray crystallography clearly reveals how the Q[*n*]s binds with 4-AP to form complexes and displays the formation of Q[5]-outer-surface complex. The macrocycles Q[6], TMeQ[6] and Q[7] formed 1:1 host and guest complexes with 4-AP respectively, while Q[8] formed a stable 1:2 ternary complex due to its large cavity, which can accommodate two 4-AP molecules. ITC data indicated that the bindings between the Q[*n*]s (Q[6], TMeQ[6], Q[7] and Q[8]) and 4-AP were mainly driven by enthalpy in these four systems and the expected high binding constant (3.684×10^{9} M^{-2}) of the supramolecular complex Q[8]@4-AP suggested that the Q[8]@4-AP ternary complex is more stable than the other four systems.

Declaration of competing interest

The authors declare that they have no known competing financial interests or personal relationships that could have appeared to influence the work reported in this paper.

Acknowledgments

This work was supported by the Innovation Program for High-level Talents of Guizhou Province (No. 2016-5657). Carl Redshaw thanks the University of Hull for support.

Supplementary materials

Supplementary material associated with this article can be found, in the online version, at doi:10.1016/j.cclet.2022.108040.

References

[1] L. Horton, A. Conger, D. Conger, et al., Neurology 80 (2013) 1862–1866.
[2] S.A. Morrow, H. Rosehart, A.M. Johnson, Mult. Scler. Relat. Dis. 11 (2017) 4–9.
[3] S.D. Broicher, L. Filli, O. Geisseler, et al., J. Neurol. 265 (2018) 1016–1025.
[4] K.C. Hayes, A.R. Blight, P.J. Potter, et al., Spinal Cord. 31 (1993) 216–224.
[5] V.I. Leussink, X. Montalban, H.P. Hartung, CNS Drug 32 (2018) 637–651.
[6] D.J. Snodin, Org. Process Res. Dev. 14 (2010) 960–976.
[7] W. Eric, Anal. Biochem. 113 (1981) 139–143.
[8] W. Zhang, Y. Luo, J. Zhao, et al., Sens. Actuat. B: Chem 354 (2022) 131189.
[9] P.H. Shan, J.H. Hu, M. Liu, et al., Coord. Chem. Rev. 467 (2022) 214580.
[10] M. Liu, L.X. Chen, P.H. Shan, et al., ACS Appl. Mater. Inter. 13 (2021) 7434–7442.
[11] D. Yang, M. Liu, X. Xiao, et al., Coordin. Chem. Rev. 434 (2021) 213733.
[12] W.T. Xu, Y. Luo, W.W. Zhao, et al., J. Agric. Food Chem. 69 (2021) 584–591.
[13] J. Lagona, P. Mukhopadhyay, S. Chakrabarti, et al., Angew. Chem. Int. Ed. 44 (2005) 4844–4870.
[14] K. Kim, N. Selvapalam, Y.H. Ko, et al., Chem. Soc. Rev. 36 (2007) 267–279.
[15] R.N. Dsouza, U. Pischel, W.M. Nau, Chem. Rev. 111 (2011) 7941–7980.
[16] B. Xiao, Y. Fan, N.N. Ji, et al., Supramol. Chem. 27 (2015) 4–12.
[17] A.E. Kaifer, Acc. Chem. Res. 47 (2014) 2160–2167.
[18] L. Isaacs, Acc. Chem. Res. 47 (2014) 2052–2062.
[19] K.I. Assaf, W.M. Nau, Chem. Soc. Rev. 44 (2015) 394–418.
[20] X. Hou, C. Ke, J.F. Stoddart, Chem. Soc. Rev. 45 (2016) 3766–3780.
[21] J. Liu, Y. Lan, Z. Yu, et al., Acc. Chem. Res. 50 (2017) 208–217.
[22] J. Murray, K. Kim, T. Ogoshi, et al., Chem. Soc. Rev. 46 (2017) 2479–2496.
[23] W. Liu, S.K. Samanta, B.D. Smith, et al., Chem. Soc. Rev. 46 (2017) 2391–2403.

[24] M.N. Sokolov, D.N. Dybtsev, V.P. Fedin, Russ. Chem. Bull. 52 (2003) 1041–1060.
[25] M. Liu, R. Cen, J.S. Li, et al., Angew. Chem. Int. Ed. 61 (2022) 202207209 e.
[26] X.L. Ni, X. Xiao, H. Cong, et al., Chem. Soc. Rev. 42 (2013) 9480–9508.
[27] M. Liu, M. Yang, Y. Yao, et al., J. Mater. Chem. C 7 (2019) 1597–1603.
[28] R.H. Gao, L.X. Chen, K. Chen, et al., Coordin. Chem. Rev. 348 (2017) 1–24.
[29] Z.C. Liu, S.K.M. Nalluri, J.F. Stoddart, Chem. Soc. Rev. 46 (2017) 2459–2478.
[30] R. Cen, M. Liu, J.H. Lu, et al., Chin. Chem. Lett. 33 (2022) 2469–2472.
[31] J.W. Lee, S. Samal, N. Selvapalam, et al., Acc. Chem. Res. 36 (2003) 621–630.
[32] M. Liu, J. Kan, Y. Yao, et al., Sens. Actuat. B: Chem. 283 (2019) 290–297.
[33] S.J. Barrow, S. Kasera, M.J. Rowland, et al., Chem. Rev. 115 (2015) 12320–12406.
[34] R.L. Lin, J.X. Liu, K. Chen, et al., Inorg. Chem. Front. 7 (2020) 3217–3246.
[35] X.D. Zhang, K. Chen, W.Y. Sun, Chem. Eur. J. 27 (2021) 5107–5119.